Evaluation of tantalum-based materials for hydrogen separation at elevated temperatures and pressures☆

Kurt S. Rothenberger[a,*], Bret H. Howard[a], Richard P. Killmeyer[a], Anthony V. Cugini[a], Robert M. Enick[b], Felipe Bustamante[b], Michael V. Ciocco[c], Bryan D. Morreale[b,c], Robert E. Buxbaum[d]

[a] *National Energy Technology Laboratory (NETL), US Department of Energy, P.O. Box 10940, Pittsburgh, PA 15236, USA*
[b] *NETL Research Associate, Chemical and Petroleum Engineering Department, University of Pittsburgh, Pittsburgh, PA 15261, USA*
[c] *NETL Support Contractor, Parsons, Inc., P.O. Box 618, South Park, PA 15129, USA*
[d] *REB Research and Consulting, Oak Park, MI 48237, USA*

Received 20 June 2002; received in revised form 7 January 2003; accepted 28 February 2003

Abstract

The hydrogen permeability of bulk tantalum and tantalum coated with thin films of palladium was measured at temperatures from 623 to 1173 K and hydrogen partial pressures from 0.1 to 2.6 MPa in a flowing gas system. Palladium coatings were deposited by both electroless plating (1–2 μm thick Pd layer) and cold plasma-discharge sputtering with two different thicknesses, 0.04 or 1.2 μm. All samples studied showed declining permeability values with surface fouling over time. The highest absolute values of permeability were observed at the lowest temperatures of study (623–773 K). However, permeability data taken at 1173 K tended to be more consistent with less scatter. The overall trend exhibited declining permeability values as a function of temperature. As confirmed by surface analysis, the palladium coating was lost from the coated tantalum samples. In one test, a 1.2 μm sputter-coated palladium film was observed peeling off the tantalum surface after 49 h at 773 K. The tantalum surface of all tested samples exhibited oxidation, distortion and cracking. Tantalum hydride formation was observed at 623 K on a palladium sputter-coated sample. Surface fouling limited the hydrogen permeability of all samples studied.
© 2003 Elsevier Science B.V. All rights reserved.

Keywords: Tantalum; Hydrogen permeability; Palladium-coated tantalum; High-temperature

1. Introduction

Improved methods for the separation of hydrogen from other gases are a key component of the US Department of Energy's "Vision 21" program. This program is charged with developing the next generation of energy plants with the goal of effectively eliminating, at competitive costs, environmental concerns associated with the use of fossil fuels for producing electricity and transportation fuels. Vision 21 does not describe a specific plant configuration, but rather it outlines a series of technology modules, or options, that would allow a plant to configure to the energy needs and available resources in a given area. However, most Vision 21 configurations incorporate a gasifier, followed at some point by the water–gas-shift

☆ Reference in this paper to any specific commercial product, process, or service is to facilitate understanding and does not necessarily imply its endorsement or favoring by the US Department of Energy.

* Corresponding author. Tel.: +1-412-386-6082; fax: +1-412-386-4806.
E-mail address: kurt.rothenberger@netl.doe.gov (K.S. Rothenberger).

reaction, resulting in a stream consisting of predominantly hydrogen and carbon dioxide that would require separation. A membrane reactor capable of handling a high-temperature, high-pressure gas stream would greatly benefit Vision 21 in that it would serve the dual purpose of enhancing conversion of carbon monoxide by selective removal of hydrogen, and separating the hydrogen and carbon dioxide products. The ideal membrane reactor would be capable of functioning in a high-temperature, high-pressure flowing gas environment so as to maximize the efficiencies of the hot, high-pressure gasifier stream and take advantage of the more rapid chemical kinetics at high-temperature [1].

Tantalum presents an intriguing possibility as a component in a hydrogen separation membrane. Its permeability to hydrogen is among the highest of any pure materials [2]. It is a mechanically tough and durable material that can easily be incorporated into a metal infrastructure over a wide temperature range. It is relatively inexpensive for a specialty metal. Compared to palladium, it is approximately an order of magnitude cheaper, and is expected to possess hydrogen permeabilities approximately an order of magnitude larger.

However, tantalum also has significant shortcomings. One major difficulty is the tendency of tantalum to form resistant surface oxide layers [3]. This has, in turn, resulted in a paucity of experimental data on tantalum-based systems.

1.1. Permeability of hydrogen in tantalum

The most commonly cited reference for the permeability of hydrogen in various materials is a comprehensive report by Steward [2]. However, it is instructive to note that Steward contains no citation of experimentally measured hydrogen permeability data for tantalum. Rather, a correlation is developed, based on the product of experimentally measured hydrogen solubility and hydrogen diffusivity data for tantalum. Specifically, for purposes of the Steward correlation, the solubility of hydrogen in tantalum was based on literature data taken from 625 to 944 K, and 0.133 to 106.7 kPa [4], expressed in the form of Eq. (1):

$$S(H_2/Ta)\ (\mathrm{mol}/(\mathrm{m}^3\ \mathrm{Pa}^{0.5})) = 0.132 \exp\left(\frac{4050}{T}\right) \quad (1)$$

The diffusivity expression used in the permeability correlation was based on a study conducted over a lower temperature range of 253–573 K [5]. This expression was cited in a critical review [6], and is shown in Eq. (2):

$$D(H_2/Ta)\ (\mathrm{m}^2/\mathrm{s}) = (4.4 \times 10^{-8}) \exp\left(\frac{-1620}{T}\right) \quad (2)$$

The data from this diffusivity study [6] was also in agreement with the results of a number of other studies [7–9], none of which went above 573 K. It is interesting to note that the review [6] excluded several sets of diffusion coefficient data [10–12], that were approximately 50% lower than the values provided by Eq. (2), even though these studies covered a wider temperature range.

In spite of the lack of overlap in the temperature ranges, the product of Eqs. (1) and (2) were used to estimate the hydrogen permeability of tantalum [2], as expressed in Eq. (3):

$$k(H_2/Ta)\ (\mathrm{mol}/(\mathrm{m\ s\ Pa}^{0.5})) = (5.8 \times 10^{-9}) \exp\left(\frac{2430}{T}\right) \quad (3)$$

It is further interesting to note that graphical representations of the correlation in Eq. (3) can be found in the literature extrapolated to 1000 K [13–16], well above the range of both the solubility and diffusivity studies.

Eq. (3) indicates that the permeability of tantalum decreases with increasing temperature because the diffusion coefficient increases with temperature more slowly than the hydrogen solubility decreases.

Measurements of the permeability of hydrogen in tantalum at high temperatures of 948–1073 K were reported by Makrides et al. [17] and expressed in the form of a diffusion constant correlation [6]. This result, Eq. (4), may be more appropriate for developing a correlation of high-temperature permeability than the low temperature correlation, Eq. (2).

$$D(H_2/Ta)\ (\mathrm{m}^2/\mathrm{s}) = (7.5 \times 10^{-6}) \exp\left(\frac{-7290}{T}\right) \quad (4)$$

The product of Eqs. (1) and (4) provide an alternate expression for the permeability of tantalum in the

temperature range of 948–1073 K.

$$k(H_2/Ta)\ (mol/(m\,s\,Pa^{0.5})) = (1.0 \times 10^{-6}) \exp\left(\frac{-3240}{T}\right) \quad (5)$$

Unlike Eq. (3), Eq. (5) indicates that the permeability of tantalum can be expected to increase with increasing temperature because the diffusion coefficient increases with temperature more rapidly than the hydrogen solubility decreases. Despite this difference in trend, the permeability values obtained using Eqs. (3) and (5) differ by a factor of less than 3 over the 948–1073 K temperature range.

1.2. Surface contamination

Except for the previously cited work of Makrides et al. [17], direct experimental measurements of the hydrogen permeability in tantalum are rare. It is expected that the calculated permeability would be difficult to attain in a real system due to the dominance of surface effects. Unlike palladium, tantalum lacks significant catalytic activity for dissociation of hydrogen molecules into atoms, a prerequisite for permeation through the material. In addition, tantalum tends to form a tenacious surface oxide layer. One author of a diffusion study went so far as to heat a tantalum sample at 2273 K and 7×10^{-8} Pa (5×10^{-10} Torr) in order to remove the surface contamination and remove the surface resistance [3].

To remedy the problem of unfavorable surface effects on permeation, composite membranes have been developed in which tantalum is coated with a thin layer of palladium. In measurements of hydrogen uptake rates on tantalum, it was observed that the deposition of even a few monolayers of palladium could dramatically enhance the kinetics of hydrogen dissolution [18]. In principle, composite membranes would take advantage of the higher permeability, lower cost, and greater mechanical strength of the tantalum core, and the catalytic activity and protection afforded by the thin, non-oxidizing palladium coating. In addition, the performance of a palladium-coated tantalum membrane would be less influenced by defects in the coating than would a permeable coating on a porous substrate, as any defect would simply render a minute area of the membrane ineffective rather than causing a leak. Such structures would seem to be economically viable, catalytically active, and durable candidates as membrane materials for high-severity hydrogen separation and membrane reactor applications.

Experimental data on a palladium-coated tantalum membrane was first published in the open literature by Buxbaum [13], who used an electroless plating method to deposit a 1–2 μm thick palladium layer on a tantalum disk. This approach was later expanded to tubular membranes and other substrates [14]. These studies employed temperatures from 600 to 700 K at low-to-moderate pressure (20–373 kPa). The permeability of the tantalum membranes under these conditions was less than the value obtained from Eq. (3). This diminished permeability was attributed to transport resistances in the Pd layer, the Pd–Ta interface and the gas phase-Pd boundary. There was a very slight increase in permeability with increasing temperature, although the investigators did not draw any conclusions from this trend.

The palladium-coated tantalum approach was further refined by the group of Dye, who performed an ion-etching procedure on thin (approximately 10 μm) tantalum foils followed immediately by sputter coating of palladium, all while the sample was being maintained under a vacuum of 10^{-4} Pa (10^{-6} Torr) [15,16]. This approach insured a highly clean surface as well as deposition of a palladium layer with particular crystallographic orientations. In these examples, the membrane was studied at temperatures from 573 to 673 K and pressures of 46 and 80–116 kPa. Permeability results were promising, but could not be compared directly with that expected for bulk tantalum, since the palladium represented a significant fraction of the total membrane thickness. The permeability increased with increasing temperature, which was again attributed to the influence of the palladium coating. Interdiffusion of the palladium and tantalum was reported at temperatures above 673 K.

1.3. Objective

In summary, tantalum would appear to be a promising material as a component in hydrogen separation membranes operating under high-temperature and high-pressure conditions. However, a number of questions remain unanswered. Although most papers on

the topic reference the correlation of Steward [2], Eq. (3), it is important to remember that it is not based on experimental permeability, but on experimentally measured solubility and diffusion coefficients, each made over limited and non-overlapping temperature ranges. Experimental measurements of hydrogen permeability studies in bulk tantalum or tantalum-based composite materials are rare and available only in limited temperature and pressure ranges. Although the use of palladium coatings has been shown to be effective in enhancing the performance of tantalum-based membranes at moderate conditions, it is not known to what degree such coatings would retain their effectiveness at elevated temperature and pressure. Therefore, the objective of this study was to evaluate the performance of tantalum and palladium-coated tantalum over a wide range of temperatures (up to 1273 K) and hydrogen partial pressures (up to 2.6 MPa) characteristic of equilibrium-limited reactions that are candidates for membrane reactors. The materials studied included bulk (uncoated) tantalum as well as palladium-coated tantalum fabricated by both electroless plating and cold plasma sputtering methods. Steady-state permeation testing in a flowing configuration was used in combination with surface characterization of pre- and post-test membranes in performing the evaluation.

2. Experimental

2.1. Membrane fabrication

Bulk tantalum membranes were fabricated by punching 16 mm diameter disks out of a 1 mm thick, 99.9% pure, tantalum sheet (Alfa Aesar). The tantalum disks were mounted in Inconel 600 alloy holders by one of the two methods: brazing or welding. The brazing configuration is illustrated in Fig. 1. After mounting, the tantalum was etched using an acid mixture of 20 vol.% HNO_3, 20 vol.% HF, and 60 vol.% H_2SO_4 and rinsed with distilled water in order to remove surface oxides and contaminants before testing and/or coating.

Tantalum membranes were coated with a thin palladium layer by either electroless plating or cold plasma sputter coating. *Electroless plating* was done at REB Research using a deposition technique developed by Buxbaum and described in a series of published results [13,14,19,20]. In this procedure, the surface of the tantalum was roughened and cleaned of oxides and oil using abrasives and detergent solutions. The tantalum surface was electrolytically hydrided with the noble metal serving as the cathode. Electroless plating was used to apply an approximately 1–2 μm thick palladium film to the tantalum surface, using hydrazine

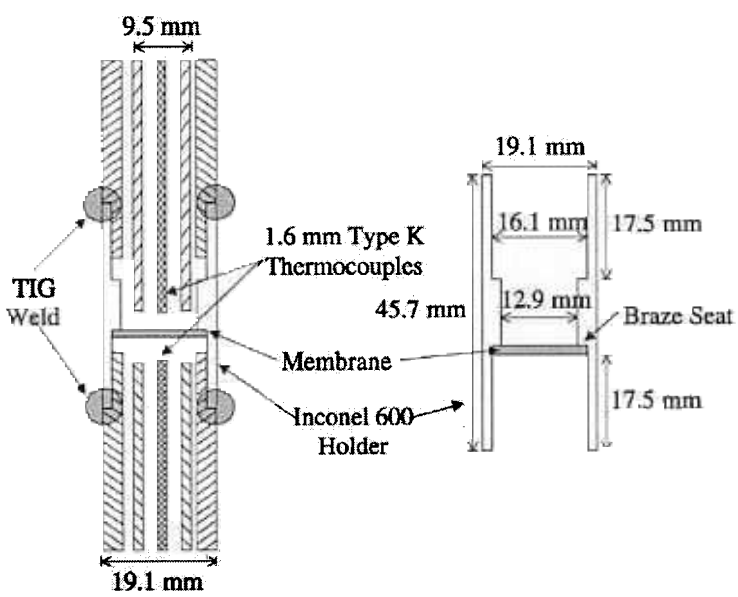

Fig. Schematic of the brazing method used for membrane sealing.

as the reducing agent rather than the hypophosphate reported in the literature. The plated metal was heated to enhance the adhesion of the palladium coating.

Cold plasma sputter-coating was done at the National Energy Technology Laboratory (NETL) using a Denton Vacuum Desk II TSC cold plasma-discharge sputter equipped with a palladium target (Alfa Aesar, 99.9% pure). Before sputtering, all surfaces except those to be coated were masked. In a typical coating procedure, the mounted membrane substrate(s) were argon etched for 60 s to remove physisorbed contaminants, and sputtered with palladium in cycles of 999 s until the desired coating thickness, either 0.04 or 1.2 μm, was obtained. The process was repeated to coat the second side of the disk. The 0.04 μm thickness was verified by performing an X-ray photoelectron spectroscopy (XPS) depth profile. The 1.2 μm coating was verified by calculation based on weight increase and by scanning electron microscopic measurement of the membrane cross-section. For the 0.04 μm coating, XPS indicated that the maximum palladium thickness was in the center of the membrane with a decrease in thickness approaching the edge, probably due to a shadowing effect of the holder walls blocking palladium deposition near the edges. This trend is expected to hold for the 1.2 μm coating, but was not measured.

2.2. Permeability testing

The hydrogen membrane testing (HMT) unit was designed and constructed at NETL and has been described previously [1,21]. The apparatus was designed to allow testing of inorganic hydrogen membranes at pressures and temperatures up to 3.1 MPa and 1173 K, respectively. A simplified schematic of the HMT unit is illustrated in Fig. 2. The membrane assembly consisted of two 9.5 mm o.d. Inconel 600 tubes, placed concentrically inside the 19.1 mm o.d. Inconel 600 extension tubes, approximately 6 mm from the membrane surface, as shown in Fig. 1. This coaxial tube configuration allowed the feed and sweep gases to enter through the annulus between the 19.1 mm o.d. and 9.5 mm o.d. tubes, contact the membrane, and exit through the inside of the 9.5 mm o.d. tube. The

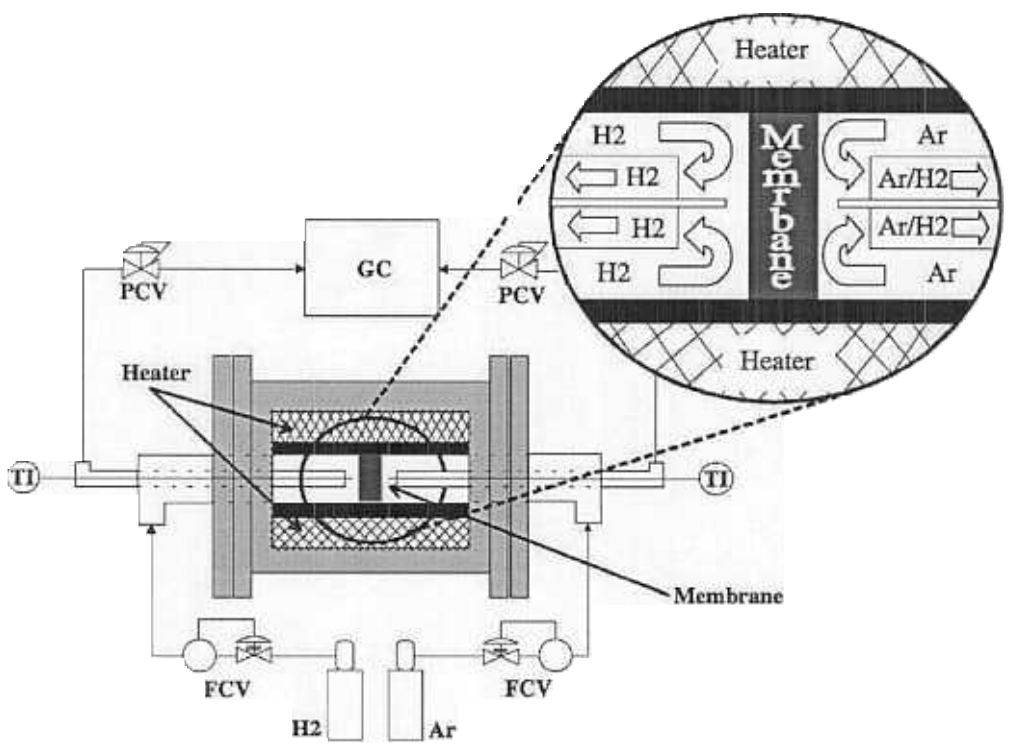

Fig. 2. Schematic of NETL's high-pressure, high-temperature hydrogen membrane testing unit.

membrane unit was heated by a Watlow 120 V, 152 mm long concentric resistance heater placed around the membrane assembly. The heater was controlled by an Iconic Genesis process control program, using type-K thermocouples placed approximately 6 mm from both sides of the membrane surface. The membrane unit and resistance heater were insulated with ceramic fiber insulation and housed inside an 8 liter stainless steel purge vessel that was continuously flushed with nitrogen. The purge vessel was used to ensure that any fugitive hydrogen evolved from the unit would be diluted, cooled, and vented safely.

The membrane unit feed gas consisted of a mixture of 90% hydrogen and 10% He while ultra-high purity argon was used for the permeate sweep gas. In some cases, the sweep gas was maintained at atmospheric pressure and the total feed pressure equaled the pressure drop. In other cases, the sweep gas was pressurized to minimize the pressure drop across the membranes. Flow rates were controlled by 5850i Series Brooks flow meters, with the feed flow ranging from 190 to 250 sccm and the sweep gas flow controlled so as to maintain the concentration of hydrogen in the permeate at generally less than 4.0 mol%. Water, hydrocarbon and oxygen traps were installed in the reactor gas inlet lines. The feed gas pressure was regulated by a pneumatic, stainless steel, Badger 807 Series Research control-valve. The hydrogen permeating through the membrane was directed to a Hewlett-Packard 5890 Series II gas chromatograph equipped with a 3 m zeolite-packed column and thermal conductivity detector. The detection of helium in the permeate gas was indicative of a membrane leak.

2.3. Permeability calculations

The hydrogen permeation rate through the tantalum membrane was determined as the product of the sweep gas flow rate and the concentration of hydrogen in the sweep gas. The hydrogen flux, N_{H_2}, was obtained by dividing the permeation rate by the surface area of the membrane. Hydrogen permeability was determined by using Eq. (6) to solve for k when the value of the partial pressure exponent, 'n', was constrained to a value of 0.5.

$$N_{H_2} = \frac{k}{X_M}(P^n_{H_2,Ret} - P^n_{H_2,Perm}) \quad (6)$$

The product of N_{H_2} and membrane thickness, X_M, was divided by $(P^{0.5}_{H_2,Perm} - P^{0.5}_{H_2,Feed})$ yielding hydrogen permeability. When a series of partial pressure data was available, k was determined by plotting N_{H_2} versus $(P^{0.5}_{H_2,Ret} - P^{0.5}_{H_2,Perm})$ and fitting with a line forced through the origin. When more than two points were available, a R^2 "measure of fit" value was also reported. In these cases, a second analysis, based on Eq. (6), was also done in which 'n' was allowed to float. In this analysis, n and k was derived from the slope and intercept, respectively, of a plot of $\log(N_{H_2})$ versus $\log(P_{H_2,Ret})$. This approach neglected the value of $P_{H_2,Perm}$.

2.4. Characterization techniques

Selected membranes were subjected to surface characterization either prior to or following flux testing (or both). Following testing, membranes were cut out of the extension tubes using a small, dry abrasive blade, taking care to control contamination. The membrane surface was photographed and examined through a stereomicroscope. Advanced instrumental characterization techniques included XPS, X-ray diffraction (XRD), and scanning electron microscopy (backscattered mode) with energy dispersive spectroscopy (SEM/EDS). In some cases, the membranes were cross-sectioned and again analyzed by SEM/EDS.

3. Results and discussion

Tantalum surfaces are well known to be fouled by oxidation and contamination by other impurities. The acid-etching technique described in Section 2 was intended to ameliorate this, so the permeability tests could at least start with a clean surface. XPS depth profiles, taken before and after cleaning, are shown in Fig. 3. Prior to cleaning, oxygen and carbon contamination levels of 10% can still be observed approximately 500 nm into the tantalum surface. Following cleaning, the XPS data shows essentially pure tantalum a few nanometers into the surface. However, it should be noted that the surface itself is still contaminated. This level of contamination is inevitable considering that the sample must be handled in air between the time it is cleaned and when it mounted in the test unit and put under inert gas.

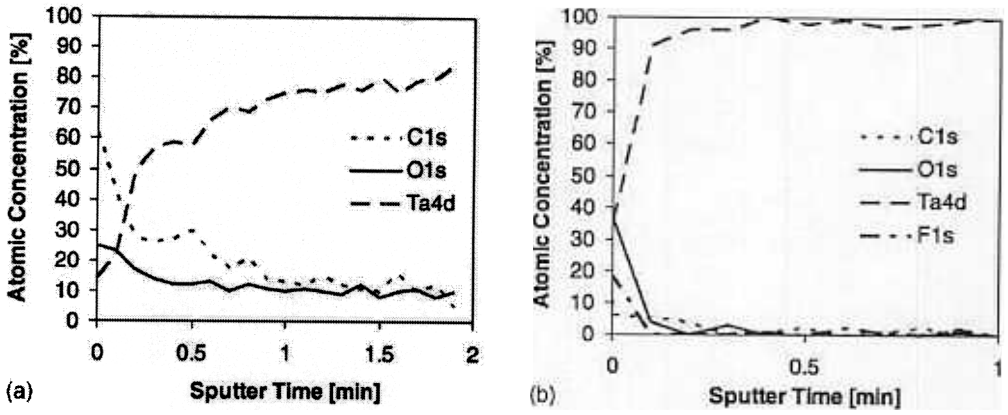

Fig. 3. XPS results on bulk tantalum surface Ta surface (a) before and (b) after "acid-etch" cleaning for 2 min in 20:20:60 nitric: hydrofluoric:sulfuric acid solution (2 min = approx. 0.5 μm in depth).

3.1. Bulk tantalum

The first bulk, uncoated tantalum membrane, designated as Ta7 in summary Table 1, was tested for hydrogen permeability for 10 days at temperatures from 873 to 1173 K and pressure drops from atmospheric to 2.8 MPa. Equilibration times were slow, particularly at the beginning of the test. On day 3 of testing, two points, at pressures of approximately 0.1 and 0.6 MPa, were recorded at a temperature of 1073 K. These points yielded a permeability of 3.7×10^{-8} mol/(m s Pa$^{0.5}$), or 66% of the value predicted from the Steward correlation.

During the 6th and 7th days of testing, a series of four partial pressure conditions ranging from 0.1 to 2.6 MPa were measured at 973 K. These values yielded consistent permeability values of 1.7×10^{-8} mol/(m s Pa$^{0.5}$) ($R^2 = 0.985$) or only 25% of that predicted from the Steward correlation. Whether this decline in permeability was due to the decline in temperature or to fouling of the membrane with time could not be determined. However, it was noted that the data at this temperature could be better fit ($R^2 = 0.996$) using an exponent of $n = 0.65$, indicating that surface effects may have influenced the permeability behavior.

During day 8 and again on day 10, data taken at 1173 K at pressures from 0.1 to 2.6 MPa partial pressure hydrogen were less consistent, although the differences in data taken on the different days was fairly minor. Overall, permeability corresponded to a value of 1.7×10^{-8} mol/(m s Pa$^{0.5}$) ($R^2 = 0.976$), essentially the same as that measured at 973 K. However, due to the decreasing nature of the Steward correlation with temperature, this value was 38% of that predicted from the Steward correlation. A better fit of the data could not be obtained by allowing the exponent, n, to float, making it difficult to determine whether the 1173 K permeability was influenced by surface effects.

During days 8 and 9, the 1073 K temperature condition was repeated, only with a wider range of partial pressures, from 0.1 to 2.6 MPa. The decline in membrane performance over time was dramatically evidenced by this result. Although the data contained significant scatter, the best fit permeability corresponded to a value of 1.3×10^{-8} mol/(m s Pa$^{0.5}$) ($R^2 = 0.903$), only 34% of the value measured during the first 3 days of testing and 22% of that predicted from the Steward correlation. The fit could be improved ($R^2 = 0.976$) using an exponent of $n = 0.77$, indicating that surface effects likely influenced the measured permeability.

A second bulk tantalum sample, designated Ta10 in Table 1, was tested for a 4-day period, at 873 K and hydrogen partial pressures from 0.1 to 1.6 MPa before a failure occurred. Measured permeability corresponded to a value of 0.94×10^{-8} mol/(m s Pa$^{0.5}$) ($R^2 = 0.888$) or only a 10th that predicted from the Steward correlation. The poor fit most likely was a result of artificially forcing the data to an exponent of $n = 0.5$. When allowed to float, a value of $n = 0.86$ improved the fit significantly ($R^2 = 0.997$), indicating that this sample was dominated by surface effects, and that the k for $n = 0.5$ is probably not valid.

Table 1
Summary of published literature data for apparent hydrogen permeability of tantalum disks

	Investigator	X_{Ta} (mm)	X_{Pd}	T (K)	$P_{Tot,Feed}$ (kPa)	$P_{H_2,Feed}$ (kPa)	$P_{tot,Per}$ (kPa)	$P_{H_2,Per}$ (kPa)	$k \times 10^8$ (mol/m s $Pa^{0.5}$)	R^2 (of $k \times 10^8$)	$k \times 10^8$ (mol/m s Pa^n)		R^2
1	Ta7 (NETL)	1	0	973	130.6–2910.5	116.0–2585.7	126.4	0.27–3.45	1.73	0.985	0.185	0.65	0.996
2	Ta7 (NETL)	1	0	1073	130.6–2903.6	116.0–2579.5	126	0.25–3.43	1.25–3.71	0.903	0.024	0.77	0.976
3	Ta7 (NETL)	1	0	1173	130.6–2931.5	116.0–2604.4	125.7–126.4	0.54–3.31	1.75	0.976	6.710	0.59	0.966
4	Ta10 (NETL)	1	0	873	106.9–1611.4	94.9–1583.7	125.7–127.1	0.08–1.70	0.94	0.888	0.0054	0.86	0.997
5	Pd/Ta (Buxbaum, 1996)	0.07–0.54	~1	693	101–303	101–303	0–150	0–150	14.50	NA	NA	NA	NA
6	Pd/Ta (Buxbaum, 1996)	NA	~1	682	20–101	20–101	~0	~0	11.00	NA	NA	NA	NA
7	Pd/Ta (Buxbaum, 1996)	NA	~1	697	20–101	20–101	~0	~0	13.00	NA	NA	NA	NA
8	Pd/Ta (Buxbaum, 1993)	2	2	616	373	280	101	5	7.50	NA	NA	NA	NA
9	Pd/Ta (Buxbaum, 1993)	2	2	630	373	280	101	5	7.90	NA	NA	NA	NA
10	Pd/Ta (Buxbaum, 1993)	2	2	644	373	280	101	5	8.80	NA	NA	NA	NA
11	Pd/Ta (Buxbaum, 1993)	2	2	658	373	280	101	5	9.80	NA	NA	NA	NA
12	Pd/Ta (Buxbaum, 1993)	2	2	671	373	280	101	5	10.70	NA	NA	NA	NA
13	Pd/Ta (Buxbaum, 1993)	2	2	686	373	280	101	5	11.60	NA	NA	NA	NA
14	Pd/Ta-electroless (NETL)	1	~1	623	106.2–106.9	94.3–94.9	127.1	0.66–0.71	1.92	NA	NA	NA	NA
15	Pd/Ta-electroless (NETL)	1	~1	923	106.2–2910.5	94.3–2585.7	125.0–127.1	0.04–0.77	0.12–0.58	0.793	0.0044	1.01	0.996
16	Pd/Ta-electroless (NETL)	1	~1	1173	106.2–1248.2	94.3–1108.9	125.7–127.1	0.14–0.18	0.38–0.39	0.911	5.95	0.46	0.896
17	Pd/Ta1-sputter (NETL)	1	~0.04	623	106.2	94.3	127.1	1.81	4.65	NA	NA	NA	NA
18	Pd/Ta2-sputter (NETL)	1	~0.04	623	104.8	93.1	127.1	3.42	12.6	NA	NA	NA	NA
19	Pd/Ta3-sputter (NETL)	1	~0.04	1173	117.0–123.0	104.9–111.1	140.0–141.0	0.69–0.74	1.83–2.28	NA	NA	NA	NA
20	Pd/Ta4-sputter (NETL)	1	~0.04	923	122.3–2845	110.0–2560	143.8–2886	0–1.63	0.04–3.88	NA	NA	NA	NA
21	Pd/Ta4-sputter (NETL)	1	~0.04	1173	120.7–2859	108.6–2573	142.7–2887	0.58–13.2	0.22–2.76	NA	NA	NA	NA
22	Pd/Ta10-sputter (NETL)	1	~0.04	623	200.6	180.5	161.3	3.44	6.38	NA	NA	NA	NA
23	Pd/Ta6-sputter (NETL)	1	~1.2	923	136.9–2896.6	123.2–2606.9	138.9–2896.6	0.22–121.22	1.16	0.954	0.108	0.65	0.997
24	Pd/Ta7-sputter (NETL)	1	~1.2	1173	139.7–140.4	125.7–126.4	138.3–139.7	2.00–2.73	1.43–2.40	NA	NA	NA	NA
25	Pd/Ta8-sputter (NETL)	1	~1.2	773	158.6–940.9	142.7–846.8	151.6–865.4	3.11–36.24	6.33–8.55	0.995	649.0	0.44	0.995

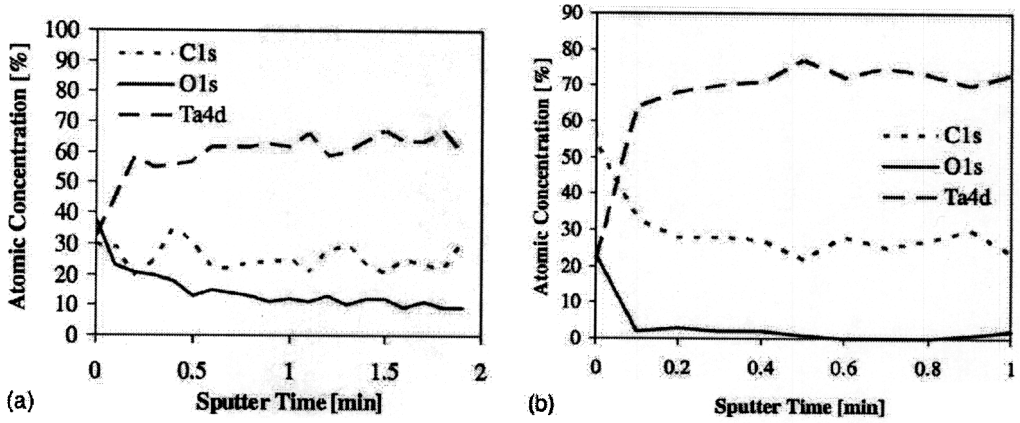

Fig. 4. XPS data on tantalum membrane after testing. Example (a) shows atomic carbon and oxygen concentrations of approximately 20 and 10%, respectively, at least 150 nm into membrane. Example (b) shows carbon atomic concentration of approximately 30% deep into membrane surface.

Surface analysis of the tantalum after testing clearly demonstrated that both membranes became contaminated over the course of the tests. XPS analysis of post-test tantalum (Fig. 4) showed carbon and oxygen levels of up to 20% at least 150 nm into the surface. This level of contamination was at least as severe as had existed in the sample before acid etching. It is possible that the high temperatures of testing caused some of the surface contaminants to diffuse further into the bulk material, resulting in a temporarily cleaner surface, but deeper bulk contamination.

SEM was also used to probe changes in surface features that occurred upon exposure to the high temperatures, pressures, and gas flows during the testing process. Following the acid etching process, some surface contour could be observed as a result of dissolution of surface Ta oxides and metal, as shown in Fig. 5a. Following testing, the surface showed a variety of changes. Specific changes observed depended on the maximum temperature, exposure duration, pressure drop across the membrane, and the side of the membrane (feed versus permeate) under examination. All bulk tantalum membranes analyzed after testing showed some degree of surface oxidation ranging from minor to extreme. Examples are shown in Fig. 5b–d.

The tantalum membrane pictured in Fig. 5b and c showed significant surface oxidation on the feed side and slightly less on the permeate side. Oxidized areas are seen as dark features in these images. A crack associated with the failure is visible in Fig. 5b. On the permeate side, evidence of surface restructuring was observed as a triangular pattern probably caused by tensional stretching of the surface due to distortion of the membrane. Oxide growth occurred preferentially at these disturbances resulting in regular tantalum oxide islands.

The membrane pictured in Fig. 5d was tested to 2.6 MPa at 1173 K. Unlike the membrane in Fig. 5b and c, this membrane exhibited no oxide phase separation. XPS depth profiling (Fig. 4) suggested the presence of carbide formation on the surface in addition to oxide. For this membrane the C and O was probably dissolved into the Ta metal. Cracking of the membrane was again seen, even though no failure occurred with this sample. The surface contamination seen in these figures most likely accounted for the drop in permeability observed after the initial 1073 K readings.

The bulk tantalum permeability results are summarized in Table 1 and Fig. 6. Table 1 also provides information on the membrane dimensions and the conditions associated with tantalum permeability values both for the NETL results and from published literature data. Fig. 6 illustrates tantalum permeability as a function of inverse temperature. Overall permeability results for bulk tantalum overlapped those published by Makrides et al., which had been measured over a similar but narrower temperature range. The temperature dependence of the NETL data was scattered, but showed a slight trend to higher permeability at increased temperature, in agreement with that recorded

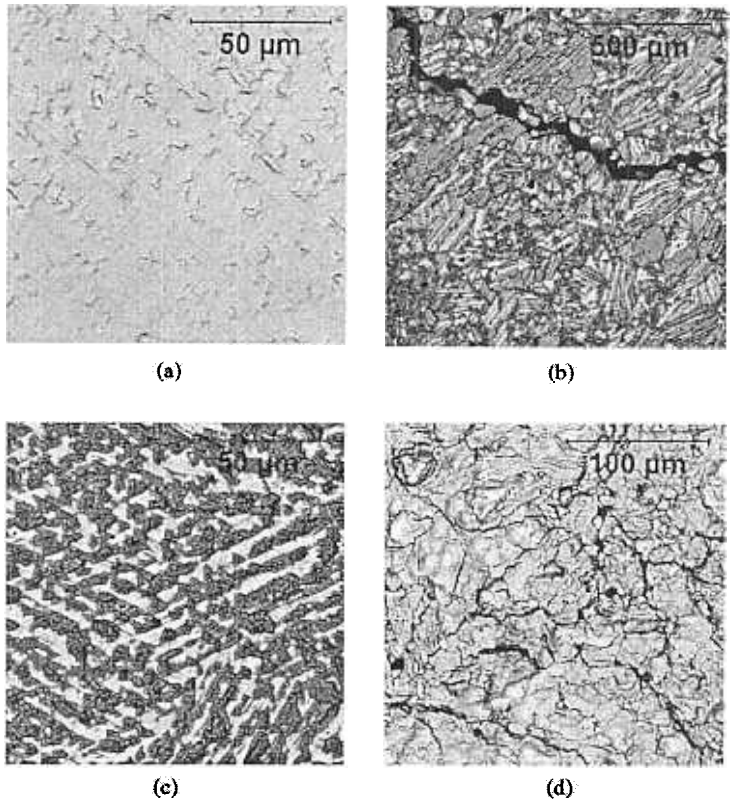

Fig. 5. SEM analysis of pre- and post-tested bulk tantalum membranes. (a) Fresh, chemically etched Ta surface showing pitting due to removal of material from the surface. (b) Feed side of post-test bulk tantalum surface showing oxidized (dark) features and crack associated with membrane failure. (c) Permeate side of post-test bulk tantalum surface showing triangular pattern indicative of tensional stretching. (d) Feed side of post-test bulk tantalum membrane showing cracking in surface.

by Makrides and opposite that predicted by Steward. Surface resistances plainly developed over time due to oxidation or contamination of the tantalum surfaces in the high-pressure, continuous-flow permeation unit. However, it also appears that surface contamination may have had a greater impact at lower temperature, thus providing some bias toward higher permeability values with increasing temperature.

3.2. Electroless-plated palladium-coated tantalum

Two electroless-plated palladium-coated tantalum membranes were prepared. One was saved for characterization, while the other was tested for 28 days, the longest single test of any tantalum-based membrane. During this time, it was subjected to temperatures of 623, 923, and 1173 K, and pressure drops up to 2.8 MPa. Equilibration times were extremely slow during the initial portion of the test. The first 17 days of testing were required to obtain just three conditions, atmospheric pressure at each of the three temperatures, with each condition requiring several days to reach steady-state operation. The initial condition, at 623 K, exhibited a slow increase in flux to an asymptotic value corresponding to a permeability of 1.9×10^{-8} mol/(m s Pa$^{0.5}$) on days 6–8. Each of the changes to higher temperature was met by an initial outgassing of hydrogen followed by an equally slow decrease in flux, again to an asymptotic value, with permeabilities of 0.58×10^{-8} mol/(m s Pa$^{0.5}$) at 923 K on day 9, and 0.38×10^{-8} mol/(m s Pa$^{0.5}$) at 1173 K on days 15–17. Each of these values is about 10% of that predicted by the Steward correlation. However, the slope of the line formed from these three initial points is nearly parallel to that of Steward.

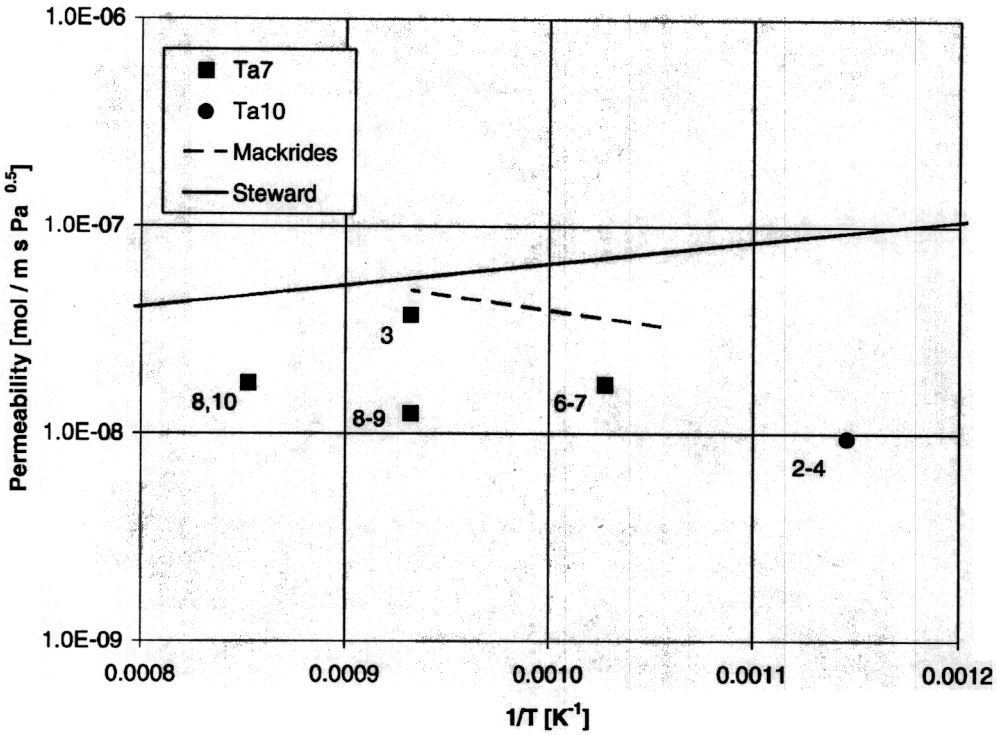

Fig. 6. Hydrogen permeability results in bulk tantalum samples. Numbers in the legend correspond to membrane designations in the text and Table 1. Numbers near the data represent the number of days into test that the data point was acquired.

Following exposure to 1173 K, equilibration times became considerably quicker, similar to that observed with the bulk tantalum samples, but measured permeabilities dropped. A return to the temperature of 923 K during days 19–20 of the test resulted in a permeability of 0.12×10^{-8} mol/(m s Pa$^{0.5}$), only 20% of its day 9 value and less than 2% of that predicted by Steward. The temperature was then raised again to 1173 K and, during days 21–26, limited pressure data was recorded from 0.1 to 1.1 MPa. Permeability values, which should have remained constant during this pressure sequence (assuming that the choice of $n = 0.5$ was a valid exponent), actually declined a total of 30% (from 0.46×10^{-8} to 0.33×10^{-8} mol/(m s Pa$^{0.5}$)) throughout this test sequence, indicating that the membrane was degrading over time. Overall, the "best fit" permeability for $n = 0.5$ was 0.40×10^{-8} mol/(m s Pa$^{0.5}$) ($R^2 = 0.911$). The fit could not be improved by a different choice of the exponent, n.

During days 27–28, a pressure study from 0.1 to 2.6 MPa was made at 923 K. Unlike the 1173 data, permeability values increased, rather than declined, over this pressure range. When forced to $n = 0.5$, the best fit permeability was 0.36×10^{-8} mol/(m s Pa$^{0.5}$) ($R^2 = 0.793$). A much better fit could be obtained with $n = 1.0$ ($R^2 = 0.996$), indicating that the membrane permeability was completely governed by surface effects at this point in the test.

Two electroless palladium-plated membranes were characterized—one in a freshly prepared state and the other following nearly a month of testing. The freshly prepared membrane, Fig. 7a and b, was fabricated by the same method as the membrane tested but was not mounted in a holder. This membrane had an estimated 80% palladium coverage on one side and significantly less on the other. The Pd had a globular appearance possibly due to growth from individual surface nucleation sites. Individual globular regions were about 10 μm in diameter. There also appeared to be some linear associations of the Pd spheres which may have been due to growth nucleation aligned with surface scratches.

Microscopic examination of the electroless-plated membrane that was removed from the reactor after

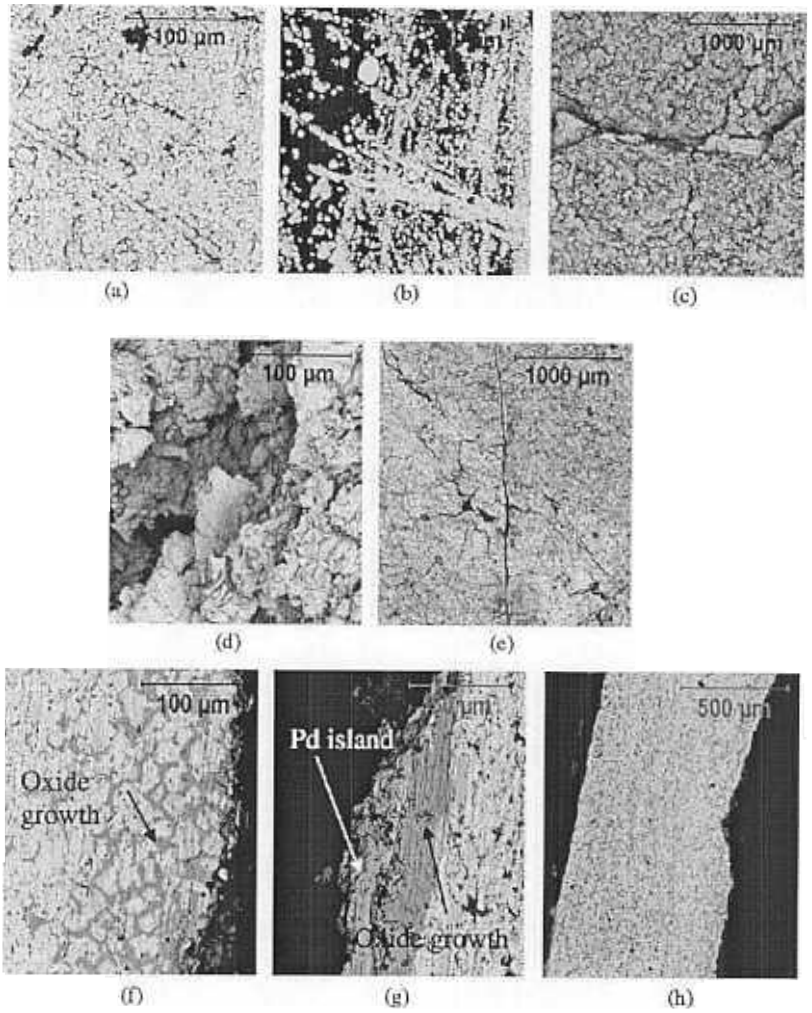

Fig. 7. SEM analysis of tantalum sample coated with 1–2 µm palladium via electroless plating. (a) Area of high Pd coverage on as-received membrane. (b) Area of low Pd coverage on as-received membrane. (c) Retentate side of membrane after testing showing surface damage. (d) Detail of the retentate side of the membrane after test. (e) Permeate side of the membrane after test showing surface damage and cracking. (f) Cross-sectional view of oxide growth into the retentate side of the membrane after test. (g) Cross-sectional view of residual palladium island and oxide growth on the permeate side of the membrane after test. (h) Cross-section of the membrane showing material loss from retentate side after test.

nearly a month of testing indicated that both the feed and sweep sides had been highly altered during membrane testing. Both sides were dark colored and rough with visible surface cracking. There was no visible evidence of palladium.

SEM/EDS results, Fig. 7c–e, suggested that the tantalum surface was oxidized and that material loss was due to spalling of this oxide layer. The surface spalling would also have removed the palladium coating. A small amount of residual palladium was found on the permeate side of the membrane although this palladium appeared very porous and poorly bound to the surface. The extreme duration of this test run as compared to others in this study accounts for the significant oxidation effects observed.

The used electroless-plated membrane was also cross-sectioned and analyzed by SEM/EDS. Examination of the feed side indicated that a tantalum oxide phase had formed in the membrane's surface, apparently forming along grain boundaries. This oxide

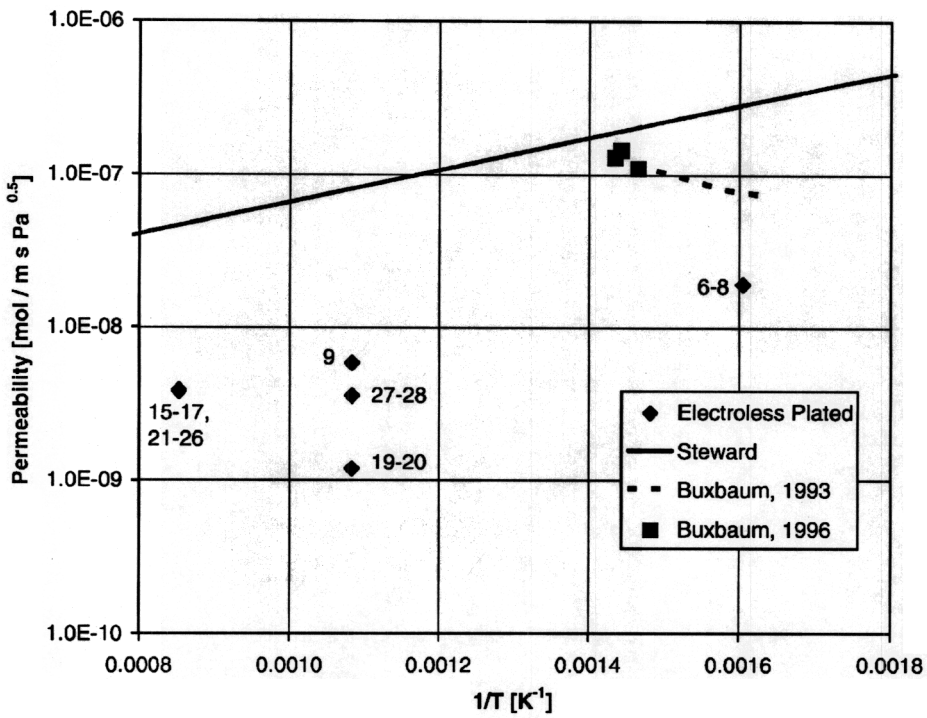

Fig. 8. Evolution of the hydrogen permeability of electroless-plated palladium-coated tantalum sample. Numbers in the legend correspond to membrane designations in the text and Table 1. Numbers near the data represent the number of days into test that the data point was acquired.

formation extended up to 200 μm into the surface, Fig. 7f.

The permeate side did not show this extreme oxide formation extending into the membrane surface. Also, there were some areas that showed residual Pd coating. One of these areas is shown in Fig. 7g. Examination of this Pd coated area indicated that the coating consisted of a somewhat porous ≈10 μm Pd layer containing some Ta and C over a similar thickness oxygen-enriched Ta layer over bulk Ta.

Also apparent from the cross-section, Fig. 7h, was that the membrane lost a large amount of material from the surface, primarily on the feed side, resulting in a reduction in thickness by about 25%. As stated earlier, this material loss was probably caused by spalling resulting from surface oxidation. The surface spalling would account for the loss of the palladium coating.

The evolution of permeability values for the electroless-plated palladium-coated tantalum membrane are shown in Table 1 and graphically in Fig. 8. These results were approximately an order of magnitude below both the Steward correlation and the data of Buxbaum and Marker [13] and Buxbaum and Kinney [14], although the temperature dependence of the permeability was fairly close to that predicted by Steward [2]. This latter fact may simply have been a result of membrane degradation over time. Due to the difficulties involved in preparing a sample at one site, coating it at another, and sending it back for mounting and testing, it is likely that the electroless-plated membrane was contaminated before the permeability test even started. The characterization data, together with permeability behavior, likely represents a consecutive series of stages involving loss of the palladium coat, fouling of the tantalum surface, spalling of the oxide layer, followed by additional fouling and loss of material.

3.3. *Sputter-coated tantalum*

As a result of difficulties encountered with the handling of the electroless-plated palladium over tantalum, it was thought that better quality control could be gained from a coating procedure done at one location.

Using the sputter coating method, the bulk tantalum metal was acid etched, placed in a vacuum chamber and ion-etched, then sputtered with palladium without removal from the chamber or exposure to air, very similar to that described in references [15,16]. Representative tantalum membranes sputter-coated with palladium were characterized before testing. For both palladium thicknesses, 0.04 and 1.2 μm, the surface morphology was not altered from that of the etched tantalum substrate. All coatings characterized appeared highly uniform.

A series of five test runs (PdTa1, 2, 3, 4, and 10 in Table 1) were made using the bulk tantalum disk sputter-coated on each side with a "thin" (average thickness = 0.04 μm) palladium film. In these tests, the sweep pressure was increased to minimize the pressure drop across the membrane. In this configuration, the partial pressure gradient is dependent on maintaining an adequate sweep flow to keep the concentration of hydrogen in the sweep gas low. PdTa1, 2, and 10 were tested at 623 K and atmospheric pressure. These runs yielded permeability values of 4.6×10^{-8}, 13×10^{-8}, and 6.4×10^{-8} mol/(m s $Pa^{0.5}$), respectively. Neglecting any contributions from the palladium film coating, these values are 16, 44, and 22% of the value predicted from the Steward correlation, and also provide a good indication of the level of variability of samples prepared using an essentially identical procedure. The value of 13×10^{-8} mol/(m s $Pa^{0.5}$) was the highest permeability measured on any tantalum-based membrane during this series of tests. In each of the tests, the membranes failed upon attempting to change temperature or pressure conditions.

Of the remaining two samples with the thin sputter-coated palladium film, PdTa3 was tested at atmospheric pressure at 1173 K. Over a 48 h period, this sample showed an initial increase in flux to a maximum value corresponding to a permeability of 2.3×10^{-8} mol/(m s $Pa^{0.5}$) (50% of the value predicted by Steward) followed by a slow decline to a steady-state value of 1.8×10^{-8} mol/(m s $Pa^{0.5}$) (40% of the Steward correlation). PdTa4 was cycled from 923 to 1173 K and back to 923 K at pressures from 0.1 to 2.6 MPa hydrogen over a 10-day period. This sample showed continuously degrading permeability behavior over the course of the test. Permeability at 923 K declined from an initial value of 3.9×10^{-8} mol/(m s $Pa^{0.5}$) (48% of Steward) on day 1 to 0.04×10^{-8} mol/(m s $Pa^{0.5}$) (<1% of Steward) on day 10. Permeability at 1173 K declined from an initial value of 2.8×10^{-8} mol/(m s $Pa^{0.5}$) (60% of Steward) on day 3 to 0.29×10^{-8} mol/(m s $Pa^{0.5}$) (6% of Steward) on day 9. No pressure dependence of the permeability could be determined due to the continuously degrading nature of the results.

After testing, no palladium could be detected on the surfaces of any of the "thin" sputter-coated membranes by XPS. Some oxidation was evident and carbon deposition was also observed. In the case of the three membranes that cracked after exposure to hydrogen at 623 K, hydride formation was suspected. However, it could not be detected by XRD for samples PdTa1 and 2. It turned out that the tantalum hydride phase was reconverting to tantalum metal upon cool down of the samples, which is usually done under inert gas following a membrane failure. In the PdTa10 test, a hydrogen atmosphere was maintained during the cool down period. Only then was the tantalum hydride phase confirmed by XRD.

Permeability values and trends are shown in Table 1 and in the plot of Fig. 9. All the points fell below the line predicted by the Steward correlation, but were much higher than those that had been obtained with the NETL electroless-plated sample. Interestingly, the values were similar to those reported by Buxbaum and coworkers in their own permeability studies of electroless-plated palladium-coated tantalum in the range of 600–700 K [13,14]. Taken together with the characterization data, the results depict a scenario where the initial permeability was high when the palladium coating was fresh (and likely intact). In the samples tested at 623 K, the concentration of hydrogen in the tantalum was high enough to form a hydride phase either before, or concomitant with, the loss of the palladium coating. In the samples examined from 923 to 1173 K, the permeability was not high enough to form a hydride. Instead, after the protective palladium coating was lost, the membrane fouled, and the permeability declined.

Subsequently, a series of three test runs, with sample designations PdTa6, 7, and 8 in Table 1, were made using bulk tantalum disks sputter-coated on each side with a "thick" (average thickness = 1.2 μm) palladium film. The goal of these experiments was to see if the palladium film thickness improved the durability of the sample or otherwise influenced the

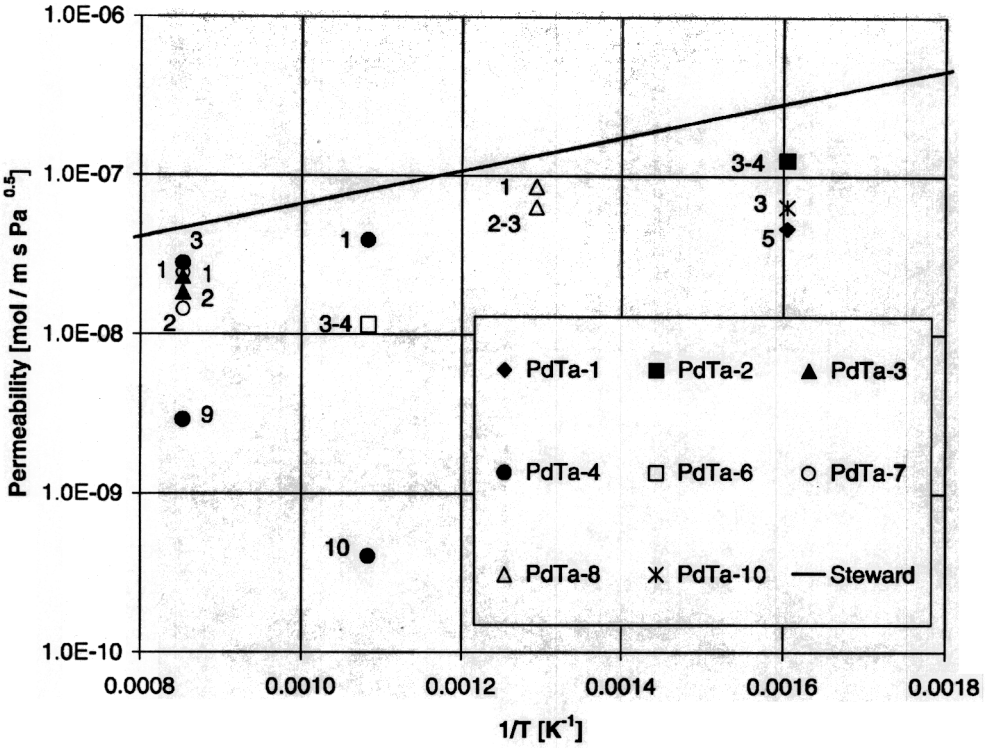

Fig. 9. Permeability of palladium sputter-coated over tantalum samples. Numbers in the legend correspond to membrane designations in the text and Table 1. Numbers near the data represent the number of days into test that the data point was acquired.

permeation behavior. Each test was limited to a single temperature to simplify the interpretation of characterization data. PdTa6 was tested at 923 K over 4 days. The sample was subjected to a complete pressure sequence from 0.1 to 2.6 MPa without any obvious degradation of the membrane over time. The permeability equation was fit to a value of 1.2×10^{-8} mol/(m s Pa$^{0.5}$) ($R^2 = 0.954$), 15% of that predicted by Steward. However, a better fit could be obtained using $n = 0.65$ ($R^2 = 0.996$), indicating that surface resistances may have been present under these conditions.

PdTa7 was tested for 48 h at 1173 K and atmospheric pressure. Measured permeability rose to a maximum of 2.4×10^{-8} mol/(m s Pa$^{0.5}$) (52% of Steward) in hour 13, then declined to a "steady-state" value of 1.4×10^{-8} mol/(m s Pa$^{0.5}$) (31% of Steward) by the end of the test. In spite of the thicker, 1.2 μm-coating, the palladium was nearly gone from both the feed and permeate surfaces of both PdTa6 and 7 after testing at 923 and 1173 K, respectively. Some minor oxidation and carbon deposition was noted. The lower degree of oxidation seen for these membranes versus previous tests was most likely due to the relatively short run duration. The limited palladium that was observed usually had a highly porous morphology. One of these residual porous-appearing palladium islands remaining on the feed side of the membrane after the 1173 K test is shown in Fig. 10a.

The PdTa8 test was designed as a short duration lower temperature exposure in an attempt to preserve the palladium coating. It took place at 773 K over 49 h. The sample showed continuous, but slow degradation of permeability from initial to final readings, from 8.6×10^{-8} to 6.5×10^{-8} mol/(m s Pa$^{0.5}$) in 5–8 h to 6.3×10^{-8} mol/(m s Pa$^{0.5}$) in 48–49 h (64–48% of Steward), with both values recorded at atmospheric pressure. A limited pressure sequence (from 0.1 to 0.9 MPa) was performed midway through the test. Only data taken during a consecutive 8 h period was included in the pressure sequence so as

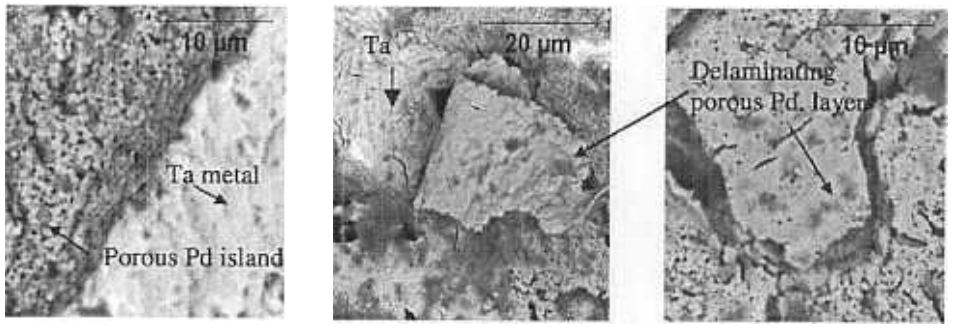

(a) (b) (c)

Fig. 10. SEM analysis of post-tested palladium-coated tantalum membrane. (a) Membrane detail showing porous palladium island remaining on tantalum substrate after 1173 K test. (b) and (c) Detail showing cracked and peeling porous palladium layer after 49 h at 773 K.

to minimize the effects of membrane degradation. This data was well fit by a permeability expression of 7.7×10^{-8} mol/(m s $Pa^{0.5}$) ($R^2 = 0.995$), 63% of Steward, and consistent with the pace of degradation over the course of the test. The fit could not be improved with the choice of a different exponent, n.

Post-test examination via SEM revealed a highly interesting observation. Palladium remained on both surfaces of the 773 K test sample. However, the palladium layer appeared cracked and porous with some areas peeling off exposing tantalum. It appeared that the conditions under which the palladium coating was lost, as well as the mechanism of its failure, had been successfully elucidated. Examples are shown in Fig. 10b and c.

The recorded permeability ranges, again with 'n' constrained to 0.5, are listed in Table 1 and Fig. 9. Taken as a group, the permeability values for both the "thin-Pd" and "thick-Pd" sputter-coated membranes fall within a range below that predicted by the Steward correlation, although many samples evidenced initial maximum readings (before degradation set in) that approached the Steward line within a factor of two. Although the highest absolute permeability values were recorded at temperatures of 723 K or less, the smaller variations in the measured permeability tended to occur at higher temperatures. This may also indicate that surface effects are less important at the highest temperatures; perhaps impurities diffuse away from the tantalum surface into the bulk material, providing at least temporary cleaning.

Based on the characterization of the fresh and tested sputter-coated membranes, particularly that for the PdTa8 sample, the palladium losses observed following testing were most likely due to delamination of the palladium layer. Although the loss of the palladium layer at elevated temperatures comes as no surprise, the mechanism was unexpected. In a previous literature reference, interdiffusion, or alloying, was cited as a cause for degradation of a sputter-coated palladium-coated tantalum sample [15]. The delamination mechanism observed in this example is consistent with our other XPS observations that were never able to detect palladium dissolved in the bulk tantalum near the surface, suggesting that alloying was not a cause of palladium loss in these studies.

Permeation data collected during testing suggested that the palladium layer survived long enough to protect the tantalum surface from oxidation during heat-up and also provided a catalytic surface that enhanced permeation until its eventual demise.

4. Conclusions

A series of bulk tantalum and palladium-coated tantalum membranes has been evaluated via direct permeability testing in a flowing system, at temperatures from 623 to 1173 K, and hydrogen pressures from 0.1 to 2.6 MPa. Membranes were characterized before and after testing so as to determine the effect of the test conditions on the sample surface.

All samples showed some degree of degradation and surface fouling, although the rates of degradation differed for individual samples. It is likely that degradation began immediately upon exposure to the

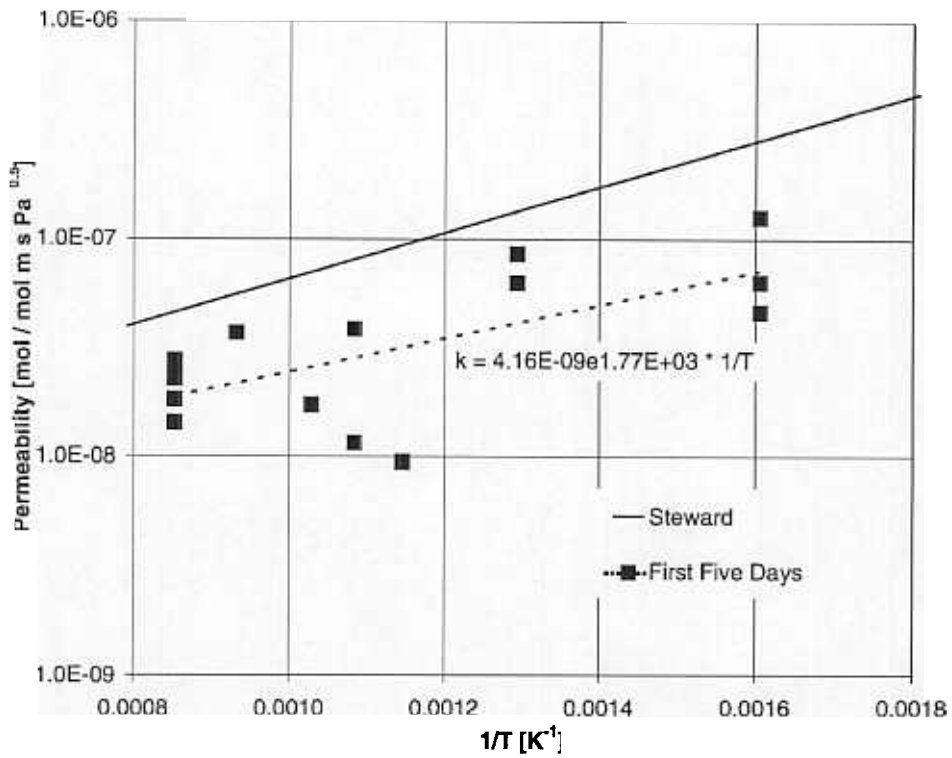

Fig. 11. Permeability values from bulk and palladium-coated tantalum recorded within the first 5 days of testing, compared to Steward correlation.

high temperatures of study, although it usually manifested itself in experimental permeability measurements within a few days.

As expected, uncoated bulk tantalum fouled relatively quickly. This, combined with slow equilibration times, made meaningful data collection difficult. The tantalum coated with a 1 μm thick layer of palladium via electroless plating exhibited strength and toughness, experiencing temperatures up to 1173 K and total pressure drops of up to 2.8 MPa over a 28-day period, but yielded the lowest overall permeabilities. This was attributed to the extensive handling that was required during preparation and coating of the sample. The sputter-coated samples gave the best overall results, at least over short periods of time.

Measured hydrogen permeabilites of tantalum and palladium-coated tantalum membranes approached, but never reached, the value predicted by the Steward correlation. The highest absolute permeability was recorded on a sputter-coated, palladium-coated tantalum sample at 623 K. This condition also corresponded with hydride formation and subsequent failure of the membrane. The highest value of permeability as a percentage of that predicted by Steward occurred before degradation of a thick sputtered palladium-coated tantalum sample at 773 K. In general, the highest temperature of study, 1173 K, provided more consistent data with less scatter and slightly higher overall permeabilities relative to that of Steward than did the lower temperature conditions.

Fig. 11 shows the permeability values of both bulk tantalum and palladium-coated tantalum samples from this study recorded *within the first 5 days of testing*. Although the choice of 5 days is somewhat arbitrary, it encompasses enough points to be representative and is a short enough time period that *significant* degradation had probably not yet set in. The resulting data, though still scattered, can be fit with an exponential expression nearly parallel to that of Steward. Table 2 lists a pre-exponential constant of 4.2×10^{-9} mol/(m s Pa$^{0.5}$) and an activation energy of -14.7 kJ/mol associated

Table 2
Pre-exponential constant and activation energy for the hydrogen permeability of bulk tantalum and tantalum coated with thin palladium films

Membrane	Data	Reference	$X_{M,Pd}$ (μm)	T (K)	k_0 (mol/(m s Pa$^{0.5}$))	E/R (K)	E (kJ/mol)	R^2
Bulk Ta	Eq. (3)	[2]*	–	253–944[a]	5.8E−9	−2430	−20.20	NA
Bulk Ta	Eq. (5)	[17]	–	948–1073	1.0E−6	3240	26.94	NA
Pd-coated Ta	Table 1 (8–13)	[13]	1–2	616–686	5.2E−6	2620	21.78	0.99
Bulk and Pd-coated Ta (first 5 days)	Table 1	This study	0–2	623–1173	4.16E−9	−1770	−14.71	0.29

Solubility and diffusivity data from temperatures of 624–944 and 253–573 K, respectively.

with the Arrhenius equation used to model the temperature dependence of this study, as well as those from previous literature references. The data shown here, in spite of the obvious shortcomings, would appear to at least qualitatively support the inverse temperature dependence of the Steward correlation over a wide range of temperature much more effectively than previous literature studies.

For the coated membranes, palladium was found to be lost from the tantalum surface for all samples studied. One particularly interesting result showed peeling and flaking palladium following exposure to 773 K for 49 h. This suggested that delamination, not interdiffusion, was the primary mechanism for palladium loss in samples at these conditions.

In spite of the efforts made to maintain a clean system, the testing was intended to simulate flowing conditions. Over the long durations of these tests, often a 100 h or more, even undetectable external leaks could have resulted in surface contamination and oxidation, which would in turn have increased surface resistance to the permeation of hydrogen. The methods employed to protect the tantalum surface from such contamination were only temporarily effective, at best, over the extreme conditions of study. As such, tantalum remains a promising material for hydrogen separation applications, but that promise will only be realized if more effective ways are found to protect the surface from fouling during the high-temperature, high-pressure, flowing gas conditions of the next generation power and energy systems.

Acknowledgements

The hydrogen membrane testing unit at NETL was operated and maintained by the Engineering Technicians of Parsons Federal Services Inc., Ronald Hirsh, Paul Dieter, Ronald Benko, Jeremy Brannen, Michael Ditillo, Stephen Lopez, Brian Neel, and Raymond Rokicki.

Nomenclature

D (H_2/Ta)	diffusion coefficient of hydrogen atom in tantalum (m^2/s)
E	activation energy for membrane permeability (kJ/mol)
k	hydrogen permeability of metal (mol/(m s Pa$^{0.5}$))
k_0	hydrogen permeability constant (mol/(m s Pa$^{0.5}$))
n	partial pressure exponent, 0.5–1.0
N_{H_2}	flux of hydrogen molecules (mol H_2/(m^2 s))
P	total pressure (Pa)
P_{H_2}	hydrogen molecule partial pressure (Pa)
$P_{H_2,Perm}$	hydrogen molecule partial pressure on permeate side (Pa)
$P_{H_2,Ret}$	hydrogen molecule partial pressure on feed side (Pa)
R	gas constant (8.314 J/(mol K))
R^2	Pearson product moment correlation coefficient
S	hydrogen solubility (m^2/s)
T	temperature (K)
X_M	membrane thickness (m)

References

[1] R.M. Enick, B.D. Morreale, J. Hill, K.S. Rothenberger, A.V. Cugini, R.V. Siriwardane, J.A. Poston, U. Balachandran, T.H. Lee, S.E. Dorris, W.J. Graham, B.H. Howard, Evaluation and